Original article
Toxicology International, *Jan-April 2017 / Vol-24 / Issue-1, 103-113*
ISSN (Print) : 0971-6580
ISSN (Online) : 0976-5131
DOI: 10.22506/ti/2017/v24/i1/149042

Toxicodynamics of Organophosphates with Human Acetylcholinesterase Interaction at Novel site Tryptophan (Trp86)

Anuj Ranjan[*1], Joyce S. F. D. de Almeida[3], Tanos C. C. França[3], Abhishek Chauhan[1], Saradindu Ghosh[2], Tanu Jindal[1*]

[1]Amity Institute of Environmental Toxicology, Safety and Management,
[2]Amity Institute of Biotechnology, Amity University, Noida, India.
[3]Laboratory of Molecular Modeling Applied to Chemical and Biological Defense (LMACBD) Military Institute of Engineering. Praça General Tibúrcio 80, 22290-270, Rio de Janeiro, Brazil
*aranjan@amity.edu

Abstract

Molecular Docking, site directed mutagenesis and molecular dynamic (MD) simulation approaches were used to explore mode of binding and inhibition for human acetylcholinesterase (*h*AChE) and organophosphates (OPs). More than 200 OPs molecules were investigated using Glide docking module of Schrodinger suite as co-crystal structure between two are not available in protein data bank. In initial screening Trp86 was found to be involved in maximum π-cation interaction on anionic subsite of *h*AChE other than Ser203 (catalytic site). With extra precision glide docking phoxim ethyl phosphonate (PEP) tops among 200 OPs based on glide docking score while interacted with Trp86, Gly121 and Ser203 whereas MM-GBSA score shows less binding affinity than heptenophos and dichlorovos. Trp86 preferred π interaction with ring bearing OPs and hydrophobic interactions with smaller OPs without ring bearing structures. Site directed mutagenesis at Trp86 (Trp86 to Ala86) shown the deterioration of the binding site in terms of size reduction, loss of electrostatic and geometric stabilization in binding cavity and significant reduction in binding of OPs in preferred orientation. Dock score of both wild and mutated *h*AChE shows a perfect qualitative agreement (R^2=64.1%) towards the study. Molecular dynamic simulation (GROMACS 4.5.5) of *h*AChE-PEP complex for 4×10^4 pico-second with SPC16 water system at 310K temperature explained the evident role of Trp86 in stabilizing the ligand at P-site of the enzyme. Asp74 and Tyr 124 were noticed in conveying H-bonds. Trp86 have shown consistent and stable distance between residues and ligand. Asp74 and Tyr124 appeared as important residues which contributed H bonds and Ser203 was expected to be closer for interaction to happen as it disappeared during simulation. Study suggests role of Trp86 on binding site is equally important to take consideration. As residue Trp86 plays significant role, it can be taken into consideration for the studies on development of more efficient antidotes to overcome the case of human poisoning.

Keywords: Docking, Molecular dynamic simulation, Human acetylcholinesterase, Organophosphates

Received: **Revised:** **Accepted:**

Introduction

Acetylcholinesterase (AChE, EC 3.1.1.7) is a serine hydrolase enzyme mainly available at neuromuscular junctions and cholinergic brain synapses. Its biological role in body is to terminate cholinergic impulse transmission by hydrolyzing the neurotransmitter acetylcholine to acetate and choline (Gabriel and Soreq, 2008). AChE is very catalytic in nature (Quinn, 1987) and being coded by AChE gene on chromosome 7 at 7q22 (Getman et al., 1992). This polypeptide has sequence of 614 amino acid length which carries signal peptide of first thirty-one amino acids. Human AChE has an ellipsoidal shape with dimensions ~ 45 Å by 60 Å by 65 Å. The enzyme

* *Author for correspondence*

is monomer and has 12 stranded central mixed β sheets surrounded by 14 α helices. The most remarkable feature of the structure is a deep and narrow gorge of ~ 20 Å long penetrating halfway into the enzyme. It widens out closer to its base which is lined with aromatic amino acids that compose various subsites (Manavalan *et al.,* 1985). The gorge is comprised of the aromatic amino acids Tyr121, Phe330, and Phe331 in *Torpedo californica*AChE (Sussman *et al.,* 1991). The hydrophobic patch contains the choline binding site and another hydrophobic site and the acyl pocket. Sussman's structure of AChE has 2.8 Å resolution on X ray diffraction provided valuable insights on many fronts. The active site of AChE lies at the bottom of a deep, narrow gorge, a substantial portion of which is lined by 14 conserved aromatic residues. AChE enzyme and its inhibitors is target to many X-ray crystallographic and molecular modeling studies. The X-ray crystal structures of AChE from different species have been documented in the protein data bank e.g. 1EVE (Kryger *et al.,* 1999).

Since the nature of cholinergic neurotransmission in the animals is ubiquitous, AChE is the target of numerous pesticides, including organophosphate and carbamate insecticides. OPs are esters or thiols derived from phosphoric, phosphonic, phosphinic or phosphoramidic acid of broad class insecticides extensively used to enhance agricultural produce and household pest control. OPs have medical importance, e.g. diisopropyl phosphorofluoridate (DFP), tetraethyl pyrophosphate (TEPP), and octomethylpyrophosphotetramide (OMPA) for the treatment of myasthenia gravis and an organophosphate esters ecothiopate, still being used to treat glaucoma(Rider *et al.,* 1951; Comroe *et al.,* 1946). They are also used as plasticizers, stabilizers in lubricating and hydraulic oils, flame retardants, and gasoline additives (De-Bleeker *et al.,* 1992).

AChE inhibition leads to accumulation of acetylcholine at the synapses causing cholinergic hyper stimulation and neurotoxicity followed by loss of metabolic balance which may lead to death in absence of any effective treatment (Haddad *et al.,* 1983). The OPs exert their main toxicological effects through non-reversible phosphorylation of esterase in the central nervous system. OPs are substrate analogues to acetylcholine and like natural substrate, enter the active site and covalently bind to serine - OH group. During acetylation, the OPssplit and the enzyme is phosphorylated, phosphate radicals of OPs bind covalently to the active sites of the cholinesterase, transforming them into enzymatically inert proteins (Worek *et al.,* 2007; Namba *et al.,* 1971). In a study by Zheng (2009) the residues Trp86, Tyr337, Phe338 and His447 are suggested as key amino acids for further study of structure-function relationships (Zheng *et al.,*2009). Recent in-silico studies also suggested active role of Trp86 in where this residue was actively involved in stabilizing the OP-*h*AChE complex through π-Cation (Ranjan *et al.,* 2015; Ranjan *et al.,* 2016).

Dephosphorylation of AChE is very slow (on the order of days), and phosphorylated enzyme cannot hydrolyze the neurotransmitter which leads to accumulation and continuous trigger the transmission of signals (Boublik *et al.,* 2002). For this reason, it is of primary pharmaceutical interest. Its inhibition is one of the most successful strategies in the reinforcement of the cholinergic transmission.

To study binding characteristics of *h*AChE, a number of ligands have been co-crystallized with the enzyme. X-ray crystallographic structure of *h*AChE with OPs has not been documented so far and further details of binding mechanism between the two are limited. This research has focused on role of active site aromatic amino acids in inhibition and binding pattern of *h*AChE with OPs. The study included random selection of seventy-five OPs commonly marketed in India, considering exposure to the population is random. Model of *h*AChE (PDB ID-1B41) was used as reference model to execute OP-*h*AChE interaction study.

Materials and Method

Preparation of protein target structure

The *h*AChE (PDB: 1B41), target protein which was complexed with a snake venom toxin fasciculin-II and other three ligands (resolution 2.76 Å) was obtained from the protein data bank in .pdb format. Structure was recovered from the model by removing crystal associated ligands hetero atoms, and water molecules. Structure was imported to Schrodinger suite, Maestro v9.5. Protein Preparation Wizard (Sastry *et al.* 2013) tool was used to optimize the structure. It comprised biological unit and assigned bond orders, zero order bonds to metals, formed disulfide bonds, deleted water molecules beyond 5 Å from hetero groups, generated metal binding states, added missing hydrogens, completed any missing side chains and loops and Protein preparation wizard.

Protein preparation wizard has a refine function, which helped in optimization of H-bond network to fix the overlapping hydrogens. pH range was established to 7.0 and the structure was minimized by applying OPLS 2005 force field (Jorgensen and Tirado-Rives 1988). Restrained minimization was used until the average root mean square deviation (RMSD) of the non-hydrogen atoms converged to 0.3Å

Receptor grid preparation

Experimental facts about the active site of AChE points out the important residues such as Ser203, Glu334, and His447. Some of the previous work on human AChE suggest that the active site consist 29 residues (Kryger *et al*. 2000 and Zheng *et al*. 2009) including the triad of Ser203, Glu334, and His447, which act as charge relay system. Binding site is composed of two different pockets connected by a narrow gorge which is lined with 14 conserved aromatic amino acids. Residues on binding site are: Gln71-Tyr-Val-Asp-Thr-Leu76, Gly82-Thr-Glu84, Trp86- Asn-Pro88, Leu130, Tyr133, Glu202-Ser-Ala204, Trp286, Phe295, Phe297, Glu334, Tyr337-Phe338, Tyr341, Trp439, His447-Gly-Tyr449, and Ile451. Grid generation was performed using OPLS_2005 force field.

Preparation of ligands

Structural files of commonly used OPs was obtained from Pubchem library (https://pubchem.ncbi.nlm.nih.gov/) (Kim *et al*., 2016). Over 200 different variant structures were used for screening. Prior to screening, preparation of OPs structures was done using LigPrepmodule (Schrödinger Release 2014) of Schrodinger suite. Ligands were imported into Schrodinger workspace and each structure was neutralized, checked for any metal binding states, desalted, generated tautomers and 32 stereoisomers per ligand was allowed. Keeping in view of the flexibility of the rings present in each ligand and their possibility to change conformations during docking calculations, we have specified to generate 1 low energy ring conformation per ligand. Finally, each ligand was energetically minimized using OPLS 2005 force field.

Virtual screening and docking

The virtual screening was performed using Virtual Screening Workflow (VSW) module of the Schrödinger Suite 2014. This workflow includes LigPrep for ligand preparation, QikProp (QikProp, version 4.0, Schrödinger 2014) to filter out ligands based on properties, and Glide docking (Friesner *et al*., 2004) at the three precision levels, high throughput virtual screening (HTVS), standard precision (SP), and extra precision (XP). HTVS and SP modes were used for a large set of ligands and XP docking is more accurate than the above two methods. After ensuring that the protein and ligands were in the correct form for docking, the previously defined binding site by Zheng et al., 2009, receptor-grid was used which includes Ser203, Glu334, and His447 forming a catalytic triad. Glide generates conformations internally and passes these through a series of filters. This first places the ligand center at various grid positions of a 1 Å grid and rotates it around the three Euler angles. In the first stage, basic score and geometrical filters eliminate unlikely binding approaches.

Second filter involves a grid-based force field evaluation and refinement of docking solutions including torsional and rigid body movements of the ligand. The final energy estimation is done with Glide Score, and a single best pose is generated as the output for a particular ligand. Glide module of the XP visualizer analyses the specific interactions. Glide includes ligand-protein interaction energies, hydrophobic interactions, hydrogen bonds, internal energy, π-π stacking interactions and root mean square deviation (RMSD) and desolvation.

G Score = a * vdW + b * Coul + Lipo + Hbond + Metal + RotB + Site

Where, vdW = van der Waal energy;

Coul =Coulomb energy;

Lipo = lipophilic contact term;

HBond = hydrogen-bonding term;

Metal = metal-binding term;

RotB = penalty for freezing rotatable bonds;

Site = polar interactions at the active site; and the coefficients of vdW and Coul are: a =0.065, b = 0.130.

All the Glide docking runs were performed on i3 Processor CPU @ 2.60 GHz, with 4 GB DDR RAM. Glide was compiled and run under Linux CentOS 6.5 operating system. The output from Glide calculations were exported to .pdb format and studied for their detailed interactions at atomic level and all the images were rendered using Schrodinger's maestro interface v9.6 and Accelry's® Discovery Studio Visualizer v 4.0 (Dassault SystèmesBIOVIA 2014).

Inducing Alanine mutation in hACHE

Based on previous studies by Ranjan et. al. (2015); Kua et al, (2003) and Ordentlich et al, (1993) which suggest significant role of Trp86 in OPs and *h*AChE interaction, another study was intended in which Trp86 was replaced with a neutral amino acid Alanine (Ala86). Mutated structure was energetically minimized and optimized using OPLS 2005 force field. Another set of HTVS was executed with same methods as discussed in previous section "Virtual screening and docking" with existing OPs ligands using virtual screening workflow (VSW) module of the Schrödinger Suite 2014. This workflow includes LigPrep for ligand preparation, QikProp to filter out ligands based on properties, and Glide docking at the three precision levels, High Throughput Virtual Screening (HTVS), Standard Precision (SP), and Extra Precision (XP).

OP ligands were screened using HTVS of Glide module in two conditions: First, binding site having Trp at 86 position (Wild *h*AChE) and second, binding site having Ala at 86 position (mutated *h*AChE). Results obtained in both cases were used to perform statistical calculations. Following energies were statistically analyzed: Dock score, Coul (Coulomb energy), Lipo(lipophilic contact term), HBond (hydrogen-bonding term) and vdW (van der Waal energy). Minitab 16.0 (Dominic, 1993) statistical software was used to do all the calculations

Molecular Dynamic Simulation

Screening of over 200 OPs led to an OP phoxim ethyl phosphonate in extra precision docking mode. The enzyme/ligand complex was simulated using the GROMACS 4.5.5 (Hess, Kutzner, Van Der Spoel, & Lindahl) package in a cubic box (742,636 nm^3) containing approximated 22.078 SPC16 water molecules with periodic boundary conditions. The minimization algorithms used were steepest descent with position restrained (PR) of ligands and protein in order to accommodate water molecules to avoid overlapping of van der Waals Radis with a convergence criterion of 100.00 $Kcal.mol^{-1}.Å^{-1}$, steepest descent without PR to flexibility the system, conjugate gradients to look for the local minimum and quasi-Newton-Raphson without PR. The minimized complex were then submitted to MD simulations in two steps. Initially, we performed 500 ps of MD at 310 K with PR for the entire system, except the water molecules, in order to ensure a balance of the solvent molecules around the residues of the enzyme. Subsequently, 40,000 ps of MD were performed at 310 K without any restriction, using 2 fs of integration time and a cut-off of 10 Å for long-distance interactions. Plots of variation of total energy, distance, the variation of RMSD and H-Bonds formed along the MD simulation were generated with the Grace program.

Results

HTVS and docking

Screening of over 200 OPs using Glide module of Schrodinger suite which performs docking at three precisions and scoring processes were used for this study. These are HTVS (high throughput virtual screening), standard precision (SP) and with extra precision (XP). SP based on Glide score criteria value allowed to pass only 13 molecules. The final docking with XP qualified only one molecule that is phoxim ethyl phosphonate.

Table 1. OPs binding with *h*AChE at standard precision docking in Glide, Top three docking score and MM-GBSA have been mentioned in bold

Organophosphates	MMGBSA-dG Binding	Docking score (Kcal/mol)
Phoxim ethyl phosphonate	-39.923	-6.247
Methamidophos	-33.207	-5.871
heptenophos	-53.017	-5.664
Fospirate	-34.948	-5.087
Dichlorovos	-41.297	-4.474
Pyridaphenthion	-33.207	-4.394
Dimefox	-38.427	-4.143
Cyanophos	-32.454	-3.969
baythion	-39.288	-3.637
Coroxon	-34.732	-3.348
Vamidathion	-38.248	-3.108
Trichlorofon	-33.207	-2.301

Top three OP based on glide docking score are Phoxim ethyl phosphonate (-6.247 Kcal/mol), methamediphos (-5.871 Kcal/mol) and heptenophos (-5.664 Kcal/mol). Phoxim ethyl phosphonate which ranked top among OPs at extra precision glide docking (-6.247 kcal/mol) however MM-GBSA binding score shows its lesser affinity (-39.923 Kcal/mol) in particular docked pose towards *h*AChE than that of heptenophos (-53.017 Kcal/mol) and dichlorovos (-41.297 Kcal/mol). Glide docking score and MM-GBSA Binding score in recorded in Table 1.

Docked files were visualized and observed in 3-D

space to study the interaction pattern. The objective during the observation was to notice the involvement and pattern of OPs with binding site residues and also with Trp86 residue of *h*AChE.

At standard precision Trp86 had shown involvement while binding with pyridaphenthion, leptophos, phoxim and phoxim ethyl phosphonate by π interactions and hydrophobic interaction of Trp86 with Trichlorofon, Vamidothion, Dichlorovos and Dimefox.

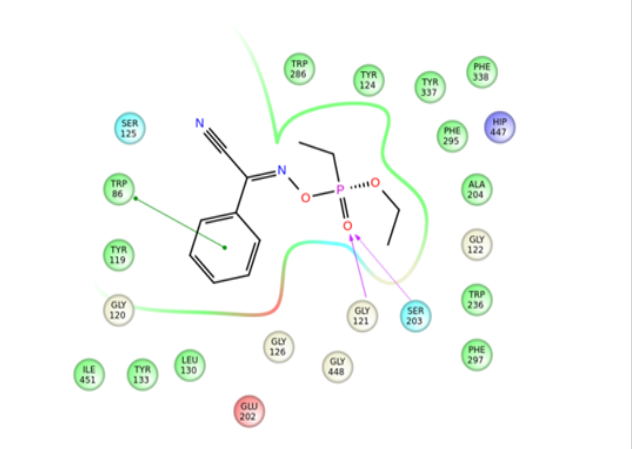


Figure 1. Phoxim ethyl phosphonate interacting with *h*AChE wild type.

Phoxim ethyl phosphonate was seen interacting with Trp86, Gly121 and Ser203 (Figure 1). Trp86 and Ser203 are believed to be the crucial residues which plays important role in the binding of OPs with AChE. Trp86 contributed π interaction. Gly120 helped in making hydrophobic contact.

Trp86 is also noticed interacting with leptophos and phoxim by π interaction as it was in case of phoxim ethyl phosphonate. Leptophos has two π contacts by Trp86 and tyr337 whereas phoxim interacted exactly as phoxim ethyl phosphonate. Ser203 has been consistent in most interactions (figure 2).

Role of Trp86 was noticeably found in stabilizing the ring containing OPs by π interaction and it was also conspicuous that smaller OPs which is not bearing any ring structure with them, Trp86 interacted with them by hydrophobic interactions. Figure 3 shows the interaction of dichlorovos, dimefox and diemethoxon with *h*AChE (wild).

In case of Pyridafenthion (Figure 4) with wild type *h*AChE, A π-πbonding is shared by Tyr124 to benzene moiety of this ligand and Ser203 to oxygen of diethoxyphosphinothioloxy group. In this binding, Trp86 is partially incorporated through hydrophobic interaction.

Effect of Trp86 to Ala86 mutation

A point mutation at Trp86 (to Ala86) shows the pose of phoxim ethtyl phosphate whichbinds with Trp86 by π interaction to benzene group of the ligand. Benzene head of the ligand immediately flips to opposite in the 3D space when Trp86 is changed to Ala86. Partial positive charge developed on the ligand was neutralized by Tyr133. Figure 5 explains the binding of Phoxim ethyl phosphonate in wild and mutated receptors model of *h*AChE.

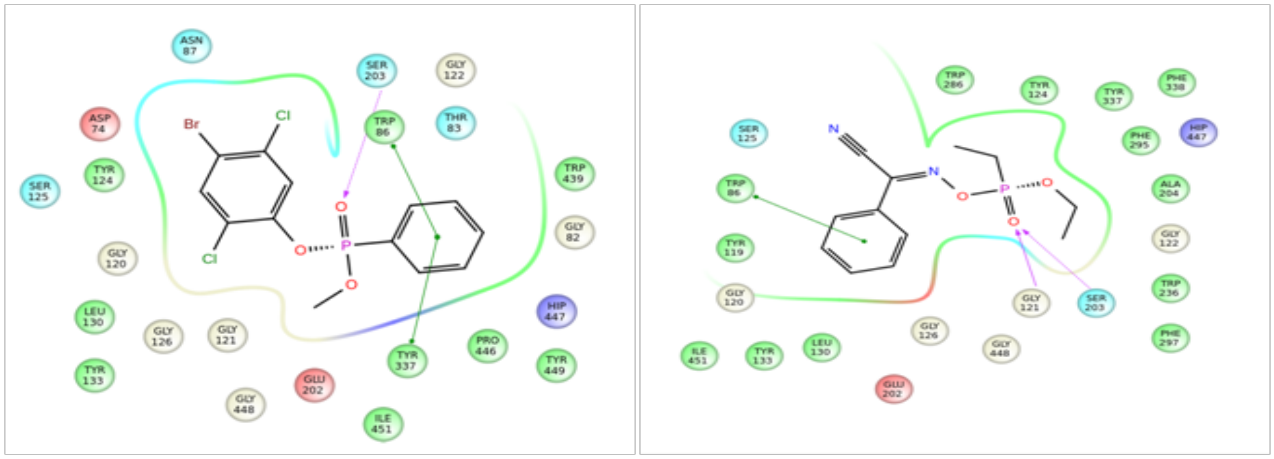


Figure 2. Leptophos interaction with wild *h*AChE (left) Benzene moiety of leptophos is being interacted with two aromatic amino acids Trp86 and Tyr337. Phoxim interacting with wild *h*AChE (right) Benzene moiety is interacting with Trp86.

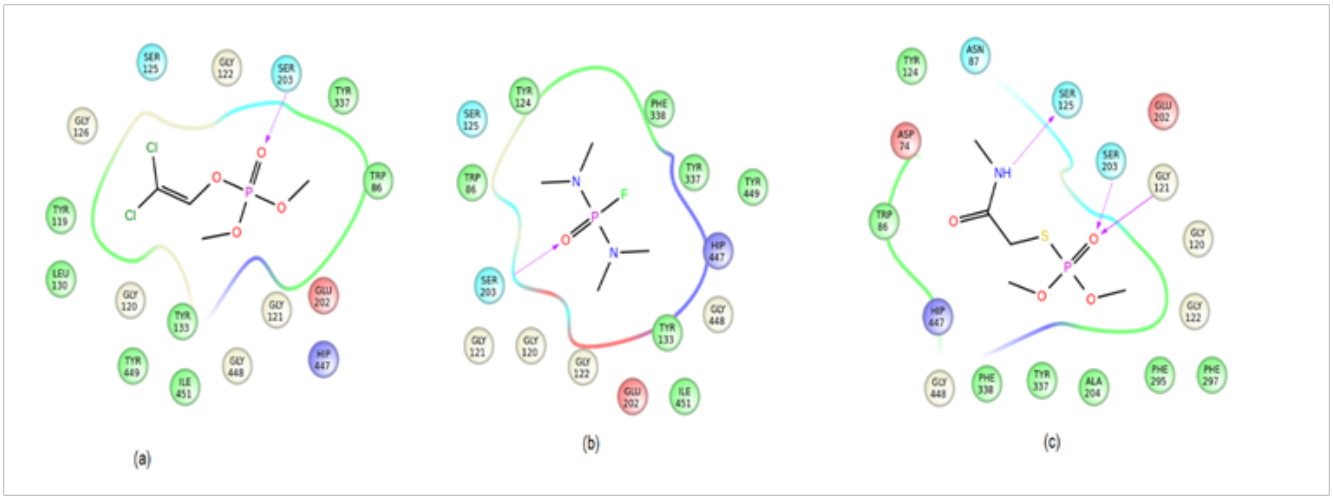


Figure 3. Binding of (a) dichlorovos, (b) dimefox and (c) dimethoxon with *h*AChE.

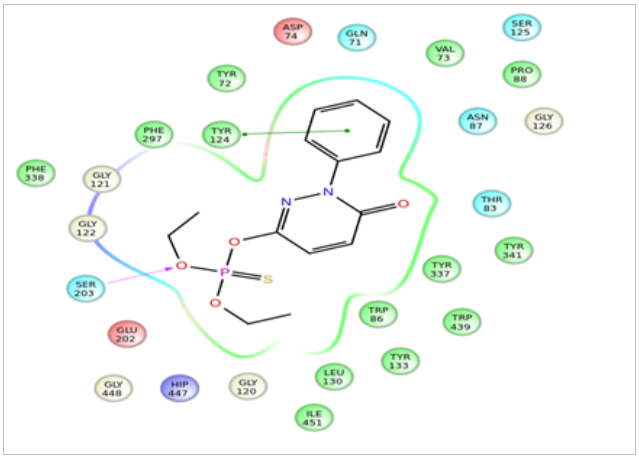


Figure 4. Pyridaphenthion interacting with *h*AChE wild and mutated type.

In case of Pyridafenthion (Figure 4) with wild type *h*AChE, A π-π bonding is shared by Tyr124 to benzene moiety of this ligand and Ser203 to oxygen of diethoxyphosphinothioloxy group. In this binding, Trp86 is partially incorporated through hydrophobic interaction. On other hand when Trp86 is mutated to Ala86; Tyr124 which was providing π-π interaction stops its contribution and Tyr341 takes this job which is situated exactly opposite to the Tyr124 in 3D space. Interaction with key amino acid Ser203 is also lost and partial positive charge generated on the molecule was normalized by π-cation provided by Phe-295 and Arg-296.

Mutation of Trp86 to Ala86 causes an electrostatic perturbation and it is noticeable that for mutation to Ala86 reduces the distances to the β-carbon and cannot

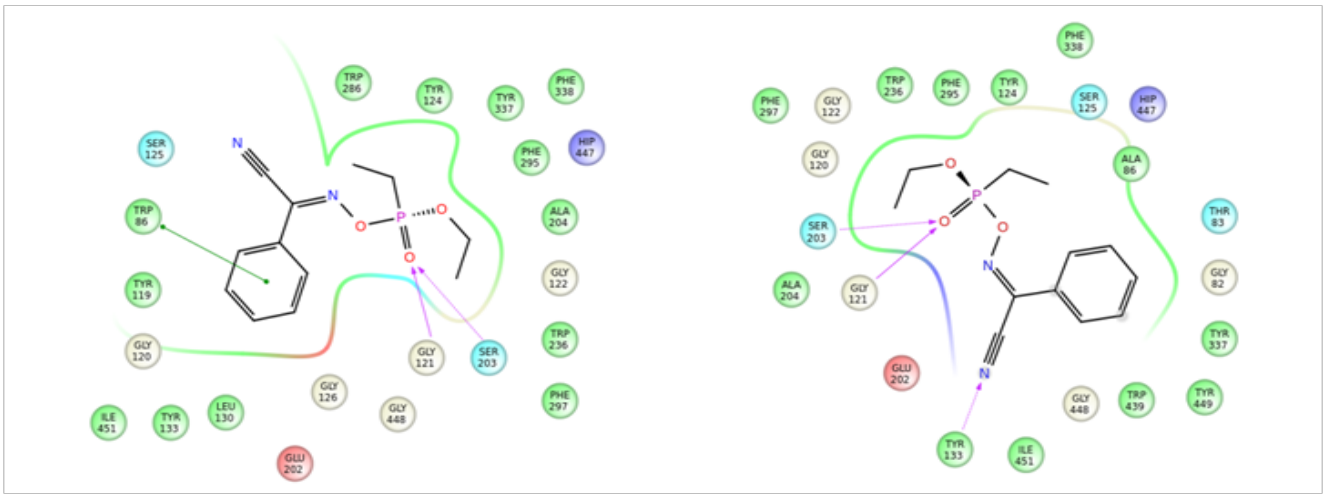


Figure 5. Phoxim Ethyl Phosphonate interacting with *h*AChE wild and mutated type.

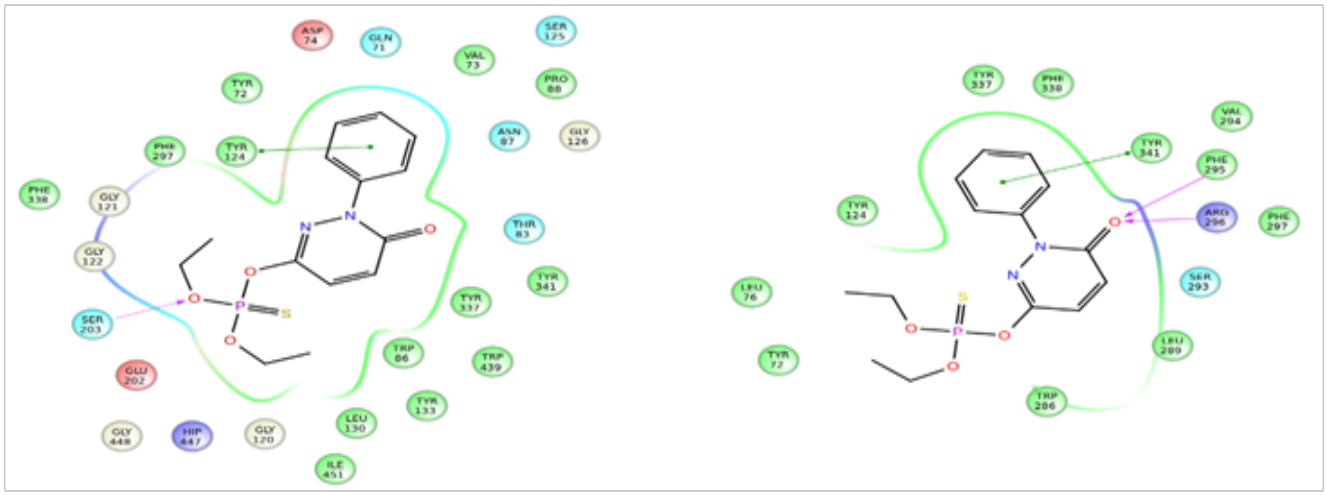


Figure 6. Pyridaphenthion interacting with *h*AChE wild and mutated type.

be compared directly with key distances to the wild state of the molecule. This also lead to change in size of reside and shape of binding site which results in reduced average docking energy.

After the Trp86 mutation, energy estimation of both wild and mutated *h*AChE in Schrodinger was done with Glide Score which includes Dock score, Coul (Coulomb energy), Lipo (lipophilic contact term), HBond (hydrogen-bonding term) and vdW (van der Waal energy) were used for Wild *h*AChE and mutated *h*AChE. Dock score shows better linear correlation with dock score of mutated *h*AChE with R^2 = 64.1% by equation:

Dock score Mutated = 0.5836 + 0.9333 × Dock Score Wild (y=mx+c)

Lipophilic contact terms (Lipo) shows moderate correlation in similar case with R-sq 51.7% by equation:

glide_lipo (mutated) = -0.3277 +0.5494 × glide_lipo (wild)

However, H bond terms shows very poor (R^2 = 8.2) and vdW (Van Der Wall energy) shows no correlation (R^2= 0.5%) at all. Figure 5 shows the linear relation of Dock score and lipophilic term contact before and after the mutation.Linear relation of dock score in wild and mutated (Trp86 to Ala86) shows the importance of Trp86 at binding cavity.

Molecular Dynamic Simulation of PEP-hAChE complex

Phoxim Ethyl phosphonate-*h*AChE complex which ranked top at XP glide docking was simulated using the GROMACS 4.5.5. The average of the total energy of the system during the simulation time was -8,13 X10-5 KJ/

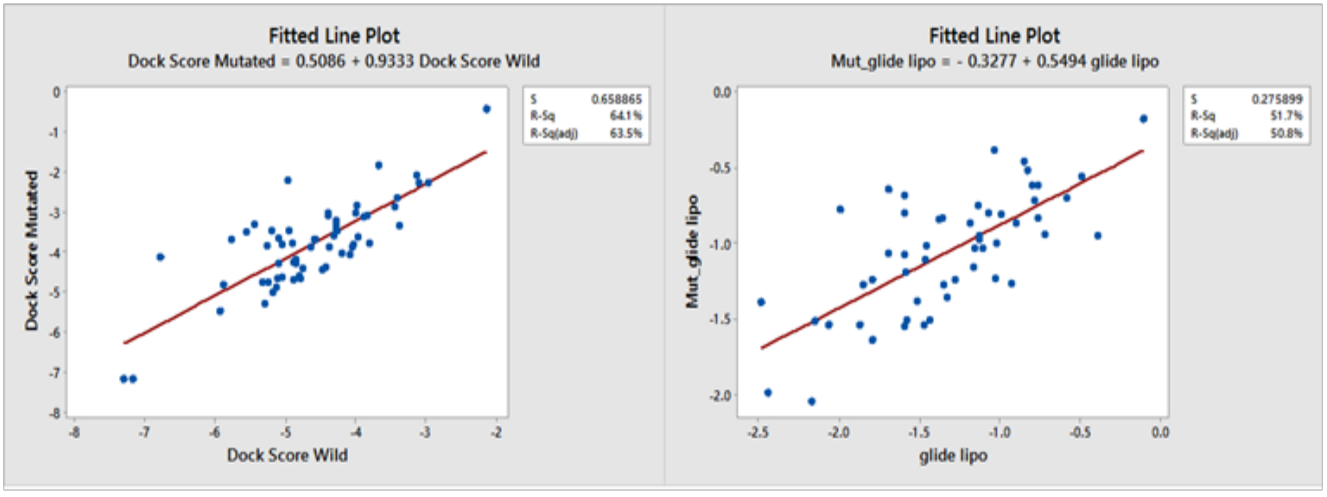


Figure 5. Correlation shows the effect of Trp86 on the binding site by comparing Dock Score and Lipophilicity.

mol (Figure 6b), with a statistic error of 130 and system stability was monitored by the RMSD values in the range of 0.52 nm (Figure 6 a).

Bond patterns

Phoxim ethyl phosphonate makes about one H-bond during the MD, but observation is not always with the same residue. At certain points of the MD, the ligand makes two bonds, but only one sustains all over the time (figure 7a). The main residues of H-bond interaction that contribute more for the stabilization of the ligand are Tyr124 (Figure 7 c) and Asp74 (Figure 7 g).

Interaction with Gly122 (Figure 7 f) and Ser203 (Figure 7 b) appear but it didin´t remain during the MD. Interaction with Gly121 (Figure 7 e) appeared in docking studies, but didn´t appear in MD. In the opposite way goes Tyr124 (Figure 7 c) and Asp74 (Figure 7 g) that didn´t appear in dockings studies but is has apppeared in MD and they are shown to be really important. Distances between the residues studied and the ligand tend to stabilize during the MD.

Distance between ligands and binding site residues

The distance Ser203-ligand showed stabilization after 10.000 ps (Figure 8 a), but showed a higher distance in comparison to docking studies. The same has occurred with Gama-oxygen of Ser203 and the P of the ligand which is about 1.13 nm (Figure 8 b). Tyr337 was observed was at the farthest (Figure 8 g). Asp74 are the closest residue (Figure 8 h). Trp86 is also closest, it also shows variation during the simulation but distance sustains in a limit. Gly121 which has appeared in the docking gets disappeared after the MD simulation. Its distance from the ligand keep increasing with the progress of the simulation.

Docking results in agreement with MD simulation of OP-*h*AChE complex strengthen the study. H bonds was largely supported by Asp74 and Tyr124. Asp74 was observed of greater importance for H-bonding as during the MD simulations Asp was most favored residue throughout the simulation, after Tyr124. H bonding with Ser203 has been reported in docking but it could not sustain during simulation reason could be the more distance between ligand and Ser203 residue. Ser203 could have been little closer for interaction to appear during the MD simulation. Trp86 shows of its greater importance as it also tends to stabilize ligands in the P-site of enzyme through π and hydrophobic interactions and distance between ligands and Trp86 was also well maintained throughout the simulation despite of several variations, the distance was falling in a certain range. Tyr337 went farthest during MD simulation and was not at enough distance to affect the ligand. MD simulation convince that the main residues that contribute to stabilization of the ligand in the hAChE sites are Asp74, Tyr124 and Trp86.

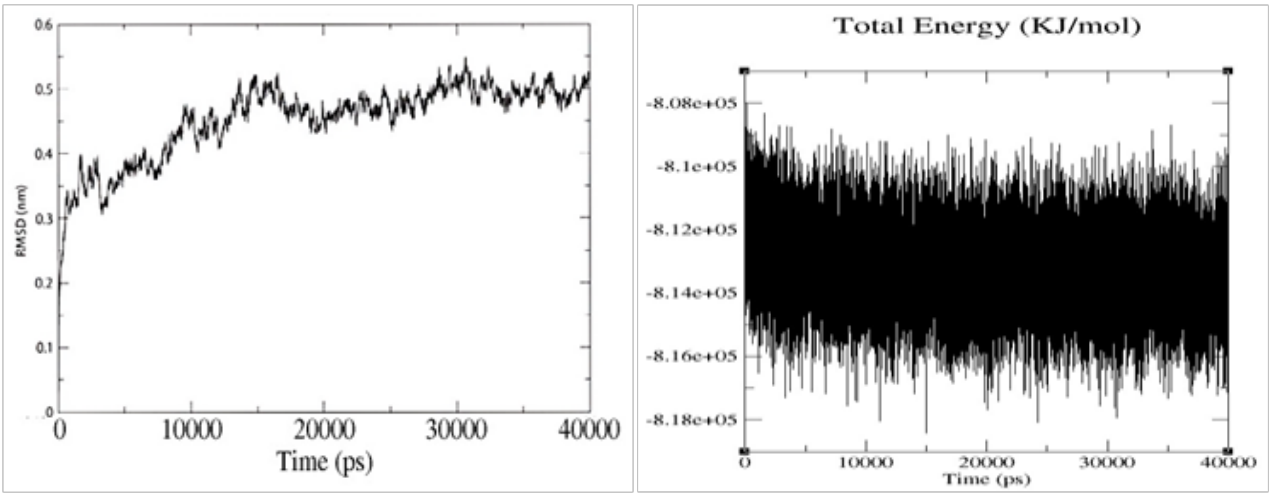


Figure 6. RMSD of PEP- hAChE complex and energy of the global system during the MD simulation upto 40000ps.

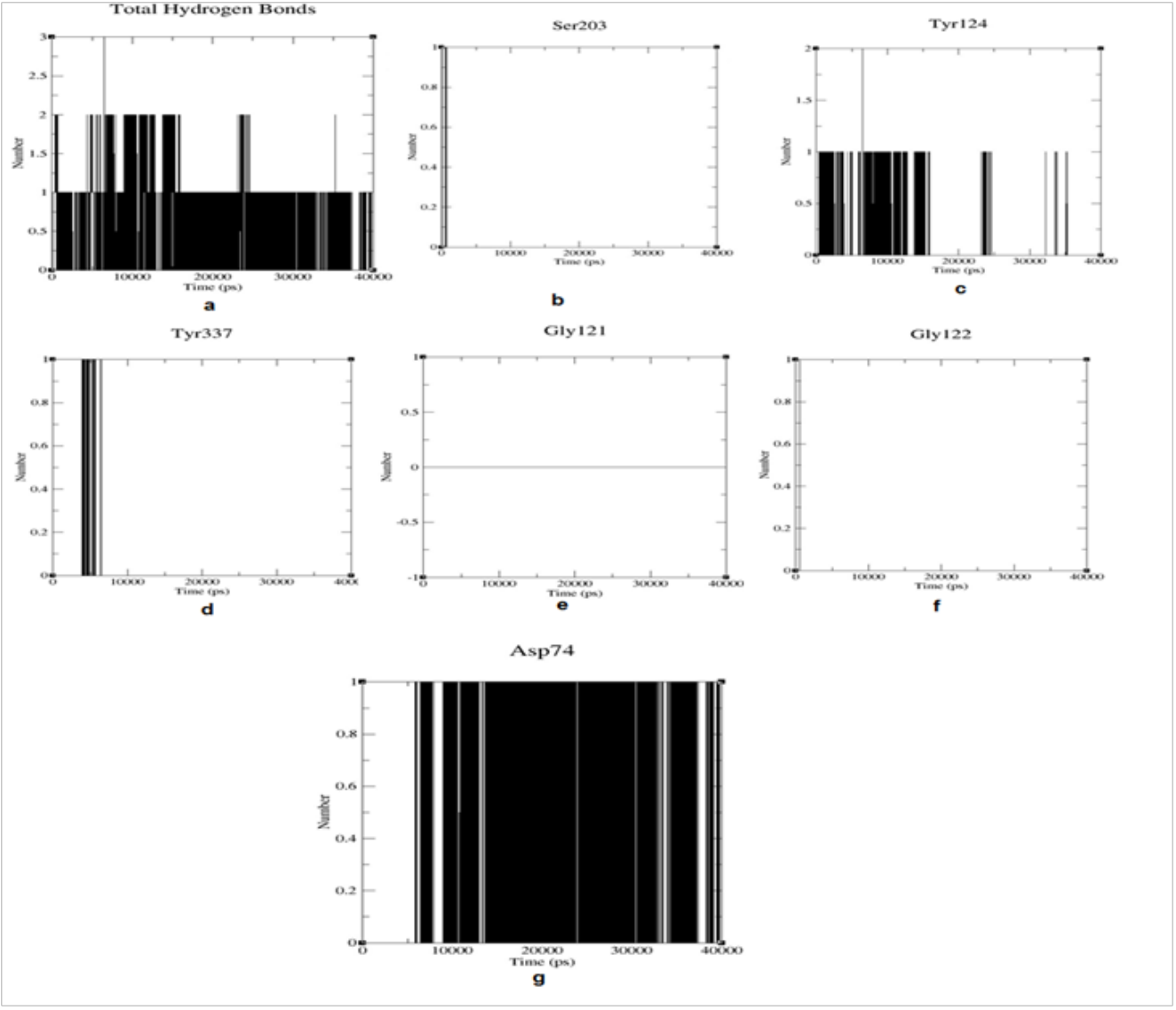


Figure 7. (a) Total number of H-bonds formed between ligands and Protein, (b-g) Behavior of H bonds formation with different residues on hAChE through out the MD simulation upto 40,000ps.

Discussion

This study infers that binding of OPs are majorly favored Ser203 (which is experimentally reported in AChE of several organisms) and Trp86. Screening of OPs on glide docking module also illustrates that OPs carrying ring structure are more likely to form π-interactions conveyed by Trp86. This residue also interacts with *h*AChE binding site by hydrophobic interaction in those OP which are not bearing any ring structure. Molecular dynamic simulation of PEP with *h*AChE helped to confirm the presence of Trp86 and Ser203 for the interaction with OPs however Asp74 and Tyr124 were helpful in contributing H bonds and H bond providers on the active site are very likely to differ with each OPs according to the functional groups present on them.

Perturbation to Trp86 results in a significant reduction in binding of OPs in preferred orientation. Trp86 has imidazole ring which makes it quite larger than Alanine. The reduction in binding energy is primarily due to size of the Trp86 residue.Changing of Trp86 residue causes large reduction in size of residue. It has a combination of effect, size reduction and loss of electrostatic stabilization in binding cavity. From an energetic point of view, due toTrp86 OPs show deterioration in docking with the mutants. This was expected that size of the cavity

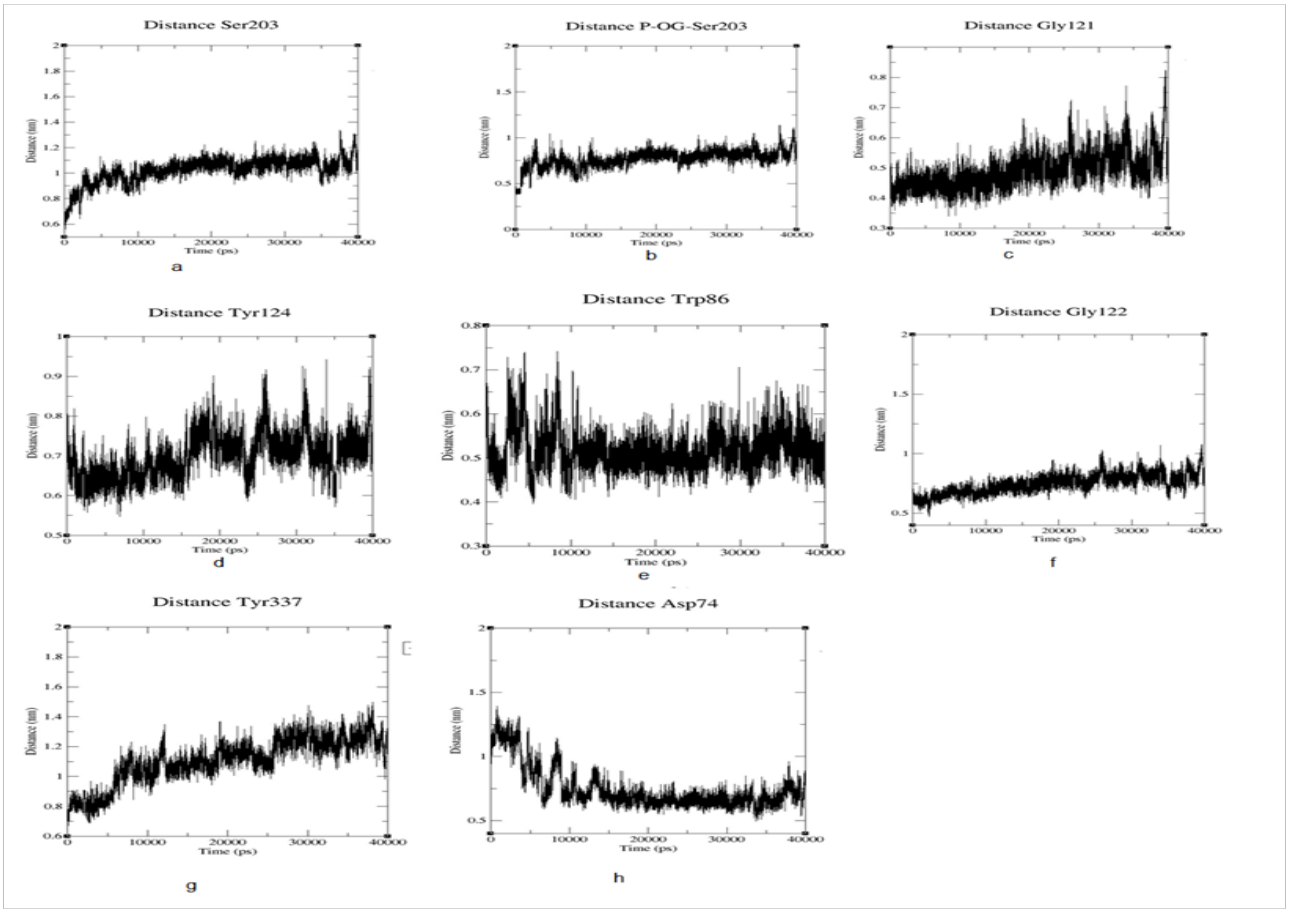


Figure 8. Distance (in nm) between various residues and ligands during the MD simulation of PEP-hAChE complex upto 40000ps.

would increase after mutating to smaller residues. The magnitude in docking energy reduction is small for any single mutation, because few subsidiary residues such as Ser203, Phe295, Arg296 and Tyr341 on binding site also support the process. It was also noticed that the docking function used underestimated the H-bond and Van Der Wall contribution. Good qualitative agreement between the obtained docking energies and lipophilicity values was found. It was also noticed in a case that charge relay center of AChE i.e. Ser203 ends its contribution after mutation. OPs having aromatic rings as head show flipped head due to poor electrostatic misbalance.

The study was supported by Zheng *et al.,* 2009 who have worked on some inhibitors used for the treatment of Alzheimer's disease have concluded the tole of aromatic residues like Trp86, Tyr337, Phe338 and His447.

Another study Lo *et al.,* 2013 performed with reactivators of tabun (an OP) inhibited AChE also enlighten the role of aromatic residues such as Trp286, Tyr337 and Tyr72 via π-π interaction. In addition to that he has also reported some interactions with the residues viz. Tyr124, Phe338, Tyr341. This study was conducted with rat AChE.

In a review ofπ-cation interactions Jennifer and Dennis (1997) have highlighted the role of π-cation interaction in the biological system and emphasized the role of aromatic residues specially Trp86 on the binding site of AChE. Role of Trp86 was again confirmed by Ordentlicha *et al.,* 2005 by studying an OP warfare agent VX, his study states that accommodation of the charged moieties of both VX enantiomers depends principally on interactions with the aromatic moiety of Trp86.

Various reports focused on Trp86 also support the present study. Shafferman *et al.*, 1992 in his work clearly states that replacement of Trp86 yielded inactive enzyme molecules. Kua *et al.,* 2003 reported the importance of Trp86 along with Glu202 and Tyr337 to have proper electrostatic balance and maintained geometry of binding gorge. Ordentlich*et al.,* 1993 reported 660 times decreased activity of enzyme after substitution of Trp86

by Alanine. Zhang *et al.,* 2003 states Combined quantum-mechanical and molecular mechanical investigation indicate a qualitative connection between specificity (or "tightness") of binding correlating with lowering of the reaction barrier.

References

1. Boublik Y, Saint-Aguet P, Lougarre A, Arnaud M, Villatte F, Estrada-Mondaca S, Fournier D. Acetylcholinesterase engineering for detection of insecticide residues. Protein Engineering 2002; 15: 43-50.
2. Comroe JH, Todd J, Gammon GD, Leopold IH, Koelle GB, Bodansky O. The effect of di-isopropylfluorophosphate (DFP) upon patients with myasthenia gravis. American Journal of Medical Science 1946; 212: 641–651.
3. De-BleekerJL, DeReuckJL, Willems JL. Neurological aspects of organophosphate poisoning. ClinNeurolNeurosurg 1992; 94(2):93-103.
4. Friesner RA, Banks JL, Murphy RB, Halgren TA, Klicic JJ, Mainz DT, Repasky MP, Knoll EH, Shaw DE, Shelley M, Perry JK, Francis P, Shenkin PS. Glide: A New Approach for Rapid, Accurate Docking and Scoring. Method and Assessment of Docking Accuracy. J Med Chem. 2004; 47:1739–1749
5. Gabriel Z, Soreq H. Termination and beyond: Acetylcholinesterase as a modulator of synaptic transmission. Cell and Tissue Research 2006; 326:655-669.
6. Getman DK, Eubanks JH, Camp S, Evans GA. Taylor P. The human gene encoding acetylcholinesterase is located on the long arm of chromosome 7. American Journal of Human Genetics 1992; 51:170–177.
7. Haddad L. Winchester J. Clinical management of poisoning and overdose. Philedelphia, WB Saunders.1983; 575-586.
8. Jorgensen WL, Tirado-Rives J. The OPLS [optimized potentials for liquid simulations] potential functions for proteins, energy minimizations for crystals of cyclic peptides and crambin. J Am ChemSoc 1988; 110(6): 1657-1666.
9. Kryger G, Harel M, Giles M, Toker L, Velan B, Lazar A, Kronman C, Barak D,. Ariel N, Shafferman A, Silman I, Sussman JL. Structures of recombinant native and E202Q mutant human acetylcholinesterase complexed with the snake-venom toxin fasciculin-II. Acta Cryst 2000; D56:1385-1394
10. Kryger G, Silman I, Sussman JL. Structure of acetylcholinesterase complexed with E2020 (Aricept): Implications for the design of new anti-Alzheimer drugs. Structure 1999; 7:297–307.
11. Kua J, Zhang Y, Eslami AC, Butler JR, McCammon JA. Studying the roles of W86, E202, and Y337 in binding of acetylcholine to acetylcholinesterase using a combined molecular dynamics and multiple docking approach. Protein Science: A Publication of the Protein Society 2003;12(12):2675-2684.
12. Lo R, Chandar NB, Kesharwani MK, Jain A, Ganguly B. In Silico Studies in Probing the Role of Kinetic and Structural Effects of Different Drugs for the Reactivation of Tabun-Inhibited AChE. PLoS ONE 2013; 8(12): e79591
13. Manavalan P, Taylor P, Johnson Jr. WC. Circular dichroism studies of acetylcholine sterase conformation. Comparison of the 11 S and 5.6 S species and the differences induced by inhibitory ligands.BBA- Protein Structure and Molecular Enzymology 1985; 829(3):365-370.
14. Namba T, Nolte CT, Jackrel J. Grob D. Poisoning due to organophosphate insecticides.Acuteand chronic manifestations. Am J Med 1971; 50: 475–492.
15. Ordentlich A, Barak D, Kronman C, Flashner Y, Leitner M, Segall Y, Ariel N,Cohen S, Velan B, Shafferman A. Dissection of the human acetylcholinesterase active center determinants of substrate specificity. Identification of residues constituting the anionic site, the hydrophobic site, and the acyl pocket. J BiolChem 1993; 268(23):17083-95.
16. Quinn DM. Acetylcholinesterase: enzyme structure, reaction dynamics, and virtual transition states. Chem. Rev 1987;87:955-979
17. Ranjan A, Ghosh S, Chauhan A and Jindal T. Molecular docking and site directed mutagenic approach to investigate the role of Trp86 of human acetylcholinesterase with organophosphates. International Journal of Pharmaceutical Science and Research 2016; 7(9): 3802-09.
18. Ranjan A, Kumar A, Gulati K, Thakur S, Jindal T. Role of Aromatic Amino Acids in Stabilizing Organophosphate and Human Acetylcholinesterase Complex. Journal of current Pharma Research 2015; 6(4): 1632-1639.
19. Rider JA, Schulman S, Richtern RB, Moeller HD, DuBois KP. Treatment of myasthenia gravis with octamethyl pyrophosphoramide; preliminary report. Journal of American Medical Association 1951; 145(13): 967-972.
20. Sastry GM, Adzhigirey M, Day T, Annabhimoju R, Sherman W. Protein and ligand preparation: Parameters, protocols, and influence on virtual screening enrichments. J Comput Aided Mol Des 2013; 27(3): 221-234.
21. Schrödinger Release 2014-2: LigPrep, version 3.0, Schrödinger, LLC, New York, NY, 2014.
22. Shafferman A, Velan B, Ordentlich A, Kronman C, Grosfeld H, Leitner M, Flashner Y, Cohen S, Barak D, Ariel N. Substrate inhibition of acetylcholinesterase: residues affecting signal transduction from the surface to the catalytic center. The EMBO Journal 1992; 11 (10): 3561 -3568.
23. Small-Molecule Drug Discovery Suite 2014-2: QikProp, version 4.0, Schrödinger, LLC, New York, NY, 2014.
24. SussmanJL, Harel M, Frolow F, Oefner C, Goldman A, Toker L, Silman I. Atomic structure of acetylcholinesterase from *Torpedo californica*: a prototypic acetylcholine-binding protein. Science1991; 253: 872–879.
25. Worek F, Aurbek N. Thiermann H. Reactivation of organophosphate-inhibited human AChE by combinations of obidoxime and HI-6 in vitro. J ApplToxicol2007; 27:582-588.
26. ZHENG QC, CHU HY, NIU RJ, SUN CC. Theoretical studies of interaction models of human acetylcholine esterase with different inhibitors. Science in China Chemistry. 2009; 52(11): 1911-1916